# Counting clusters on a grid

An illustrated, repaired draft

Jacob Richey + ChatGPT

November 2, 2026

**Abstract**

Color each vertex of the square lattice black or white independently, with equal probabilities. How many black clusters are there per unit area? We give a self-contained treatment of the limiting density, its description by reciprocal cluster size, and a method that bounds it between differences of free and wired strip rates. The bounds converge monotonically and can be computed using finite connectivity-state Markov chains. A reproducible calculation with certified arithmetic gives $0.06576983 \le \lambda \le 0.06577780$. The resulting window has width less than $8 \cdot 10^{-6}$. An Euler-characteristic identity gives a second description and a short analytic lower bound. This note revisits Richey's 2014 undergraduate thesis, retaining its central strip construction while correcting arguments, formulas, and numerical claims.

**About this version.** The original thesis was written by Jacob Richey at Dartmouth College under Peter Winkler's supervision. This repaired working draft was prepared in conversation with ChatGPT in November 2026. ChatGPT generated the initial replacement proofs, verification code, and prose; Jacob initiated and directed the revision. Full mathematical review by Jacob remains pending. The 2014 thesis is preserved as a separate document.

## 1 The question and the counting convention

### 1.1 A checkerboard question

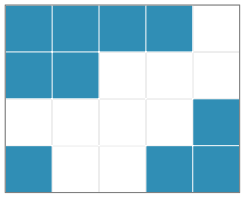
The starting point is a 2005 Putnam problem: a rectangular checkerboard is colored independently with two equally likely colors, and one is asked to show that the expected number of monochromatic regions exceeds one eighth of its area. The problem invites a more precise question: what fraction of the area is the expected number of regions, on a large board?

A region is connected through shared edges. Two squares that touch only at a corner belong to different regions unless there is another path joining them. We pass freely between this picture and a graph: put a vertex at the center of each square, and join centers of squares sharing an edge. Occupying a vertex means coloring it black. Thus the randomness is on *sites*, rather than independently on edges.

Let

$$B_{m,n} = \{1, \dots, n\} \times \{1, \dots, m\}$$

with nearest-neighbor edges. A black cluster is a connected component of the subgraph induced by the black vertices. Write $K_{m,n}$ for the number of black clusters and $e(m, n) = \mathbb{E}K_{m,n}$.




cluster sizes $1, 3, 6$ total weight $1 + 1 + 1 = 3$

Figure 1: Blue squares represent black sites. There are three black clusters. On the right, each black square receives the reciprocal of its cluster's size; each white square receives zero. Every cluster then has total weight one, irrespective of its area.

Throughout the main argument, each vertex is black with probability $1/2$, independently. We count *black clusters only*: the expected total for both colors is $2e(m, n)$.

The limiting constant is

$$\lambda = \lim_{m,n\to\infty} \frac{e(m,n)}{mn}. \tag{1.1}$$

Both dimensions tend to infinity, with no restriction on their relative rates. The existence of this limit is proved below. In the percolation literature it is the square-site cluster density at occupation probability one half. Ziff, Finch and Adamchik reported the Monte Carlo estimate $0.0657703 \pm 0.0000002$ in 1997 [2, eq. (14)]; the uncertainty in that statement is statistical. The enclosure in this draft instead comes from deterministic bounds and integer error certificates.

### 1.2 What the bounds mean, and how to read this paper

An enclosure $[L, U]$ means a proved pair of inequalities $L \le \lambda \le U$. Its *width* is $U - L$. This is different from the number of digits printed in $L$ and $U$: computing an endpoint to ten decimal places does not give a ten-decimal-place determination of $\lambda$. We will separately control the error in each finite calculation and the error from observing only a strip of the lattice.

The quantities that recur throughout the paper are collected here.

| Symbol | Meaning |
|---|---|
| $e(m, k)$ | Expected black clusters in $m$ rows and $k$ random columns |
| $e^w(m, k)$ | The same count with one extra, all-black left column |
| $a_k,\ b_k$ | Corresponding expected clusters per row in a long strip |
| $L_k = a_k - a_{k-1}$ | Lower bound on the two-dimensional density |
| $U_k = b_k - b_{k-1}$ | Upper bound on the two-dimensional density |
| $\lambda$ | Black clusters per site when both dimensions grow |

The two letters $m$ and $k$ have different jobs in a strip computation: $m$ tends to infinity, while $k$ is held fixed. Later $k$ increases to improve the bounds. Keeping these two limits separate is essential.

Section 2 explains why a density exists and what it means probabilistically. Section 3 develops the strip comparison, beginning with an example of why a new column can *decrease* the cluster count. Section 4 explains both the finite computation and its arithmetic certificate. Section 5 supplies a different, geometric description through holes and Euler's formula. The remaining sections treat the variants in the original thesis and record precisely what was checked.

The central construction comes from the 2014 thesis [1]. Observing only a finite strip leaves some connectivity outside that strip unknown. Treating all possible external connections as absent or present bounds the effect of adding the next column. This idea survives the repair. The two-dimensional constant is unchanged by periodic boundary conditions, but fixed-width strip rates are sensitive to them.

# 2 Density and reciprocal cluster size

## 2.1 Give each cluster one unit of mass

Counting clusters looks global: deciding whether two black sites belong together may require following a long path. There is nevertheless a simple way to turn a cluster count into an average over sites. Divide one unit equally among the sites of each cluster. A cluster with six sites contributes six copies of $1/6$; a singleton contributes one copy of 1. Figure 1 is the finite version of the idea.

It is convenient here to allow any occupation probability $p \in [0,1]$. For a finite set $B$, let $C_B(v)$ be the black cluster of $v$ inside $B$. Set

$$f_B(v) = \begin{cases} |C_B(v)|^{-1}, & v \text{ is black,} \\ 0, & v \text{ is white.} \end{cases}$$

For the infinite-lattice cluster $C(v)$, use the same convention and assign reciprocal size zero to an infinite cluster.

**Theorem 2.1.** *For square-site percolation at probability $p$, the density exists and is*

$$n_{\square}(p) = \lim_{m,n\to\infty} \frac{\mathbb{E}_p K_{m,n}}{mn} = \mathbb{E}_p f_{\mathbb{Z}^2}(0). \tag{2.1}$$

*In particular,*

$$\lambda = \frac{1}{2}\mathbb{E}\left[\frac{1}{|C(0)|}\,\middle|\, 0 \textit{ is black}\right]. \tag{2.2}$$

*Proof. First count inside a finite box.* Every finite black cluster contributes one to the sum of the reciprocal sizes of its vertices. Thus, configuration by configuration,

$$K_B = \sum_{v\in B} f_B(v). \tag{2.3}$$

This identity includes clusters cut apart by the boundary: each piece is counted once as a cluster of the induced graph on $B$.

*Next compare three observation windows.* Let $Q_r = [-r,r]^2 \cap \mathbb{Z}^2$, and suppose $v + Q_r \subset B$. The clusters containing $v$ are nested:

$$C_{v+Q_r}(v) \subseteq C_B(v) \subseteq C(v).$$

Their reciprocal sizes have the opposite order,

$$f_{\mathbb{Z}^2}(v) \le f_B(v) \le f_{v+Q_r}(v). \tag{2.4}$$

The inequalities also hold when $v$ is white, since all three terms are zero, or when $C(v)$ is infinite, since the left term is then zero.

*Only sites close to the box boundary need separate treatment.* Let $I_r(B) = \{v \in B : v + Q_r \subset B\}$, and write $\eta_r(B) = 1 - |I_r(B)|/|B|$. All the variables above lie in $[0, 1]$. Taking expectations in (2.3), using translation invariance in (2.4), and bounding the remaining sites by one gives

$$\mathbb{E}_p f_{\mathbb{Z}^2}(0) \le \frac{\mathbb{E}_p K_B}{|B|} \le \mathbb{E}_p f_{Q_r}(0) + \eta_r(B).$$

For a rectangle of side lengths $m, n$, and fixed $r$, $\eta_r(B) \le 2r/m + 2r/n$ once both sides exceed $2r$. Thus this error vanishes as *both* sides grow, regardless of their relative speed.

*Finally enlarge the local window.* As $r \to \infty$, the sets $C_{Q_r}(0)$ increase to $C(0)$: every finite path from 0 lies in some $Q_r$. Their reciprocals therefore converge to $f_{\mathbb{Z}^2}(0)$, including when the limiting cluster is infinite. Bounded convergence gives $\mathbb{E}_p f_{Q_r}(0) \to \mathbb{E}_p f_{\mathbb{Z}^2}(0)$. First letting $m, n \to \infty$ and then $r \to \infty$ squeezes the liminf and limsup to the same number. At $p = 1/2$, conditioning on whether the origin is black proves (2.2). □

The same proof applies to the finite-range adjacency rules used later. It does not require the absence of an infinite cluster. At $p = 1/2$ on the square lattice all clusters are finite: this is below the square-site threshold $p_c > 0.556 > 1/2$ [10].

The existence of the cluster density is classical. Grimmett proved, in particular, almost-sure and mean convergence for expanding square-site rectangles [7]. Our elementary argument above proves the expectation limit needed here and also identifies its value.

## 2.2 A typical cluster and the cluster of a typical site

There is an equivalent root description. Give each finite black cluster its lexicographically smallest vertex as a root. Sending unit mass from that root equally to the vertices of its cluster, and using translation invariance and Tonelli's theorem, gives

$$\lambda = \mathbb{P}(0 \text{ is the root of its black cluster}). \tag{2.5}$$

Here is the mass calculation explicitly. For a finite black cluster with root $x$, let $T(x, y) = 1/|C(x)|$ for $y \in C(x)$, and set $T(x, y) = 0$ otherwise. The total sent from 0 is the indicator that 0 is a root; the total received at 0 is $f_{\mathbb{Z}^2}(0)$. Translation invariance gives $\mathbb{E}T(0, y) = \mathbb{E}T(-y, 0)$. Summing these nonnegative quantities over $y$ proves equality of the expected mass sent and received, which is (2.5). The lexicographic choice commutes with translations, which is the property needed in this argument.

This is an intensity of roots, not a reciprocal of the expected size of the cluster of an occupied vertex.

To make that distinction explicit, let $n_s$ be the density of clusters of size $s$. Then

$$\lambda = \sum_{s \ge 1} n_s, \qquad \mathbb{P}(|C(0)| = s \mid 0 \text{ black}) = 2sn_s. \tag{2.6}$$

The distribution of the size of a cluster sampled by its root is $n_s/\lambda$, whose mean is $1/(2\lambda)$. Sampling an occupied vertex instead weights that distribution by size. A cluster of size six is six times as likely as a singleton to be encountered by choosing a uniform occupied site; it has no such advantage when we choose a root. This is the distinction behind the two different means.

The infinite line gives a useful numerical check. A run of $s$ occupied sites has a vacant site at each end, so its density at $p = 1/2$ is $n_s = 2^{-s-2}$. The run density is $\sum_s n_s = 1/4$. Consequently

$$\mathbb{P}(\text{root-sampled size} = s) = 2^{-s}, \qquad \mathbb{P}(|C(0)| = s \mid 0 \text{ black}) = \frac{s}{2^{s+1}}.$$

Their means are respectively 2 and 3. Their difference is already visible in one dimension; it cannot be repaired by taking a larger box. The reciprocal-size formula is consistent with both distributions:

$$\frac{1}{2}\sum_{s\geq 1}\frac{1}{s}\frac{s}{2^{s+1}} = \frac{1}{4}.$$

Counting paths also does not count clusters: several self-avoiding paths may reach the same vertex. A sum of path probabilities needs an explicit rule for removing that overcount before it can represent a cluster size.

### 2.3 A second proof by cutting rectangles

There is another useful route to the limit, because it supplies an infimum formula that we will use for strips. For later use, cutting a rectangle into two pieces gives

$$e(m, n_1 + n_2) \leq e(m, n_1) + e(m, n_2). \tag{2.7}$$

Indeed, deleting the edges across a cut cannot decrease the number of components. After the cut, the total count is the sum of the counts in the two pieces. Taking expectations proves (2.7); no independence across the cut is needed for this inequality. The same argument works in the other coordinate.

Fix positive integers $a, b$. Write $m = qa + r$ and $n = tb + s$, where $0 \leq r < a$ and $0 \leq s < b$. Cut off $qt$ disjoint $a$-by-$b$ blocks. The uncovered sites lie in two boundary strips, whose total area is at most $rn + sm$. Since a set cannot have more occupied clusters than sites,

$$e(m, n) \leq qt\, e(a, b) + rn + sm.$$

After division by $mn$ and passage to the limit, the last two terms vanish and the first tends to $e(a, b)/(ab)$. Thus the limsup of the normalized count is at most every such finite-box value. The liminf is at least their infimum, simply because every normalized finite-box count belongs to the set over which the infimum is taken. Hence

$$\lambda = \inf_{a,b\geq 1} \frac{e(a, b)}{ab}. \tag{2.8}$$

This is the rectangular Fekete argument; there is no need to exchange a joint limit with iterated limits without justification.

## 3 Bounds from free and wired strips

### 3.1 Why increments reveal the bulk density

A long strip has extra clusters near its two sides, where connections have been cut off. Dividing its count by its width therefore leaves a boundary contribution. The thesis's idea is to compare

neighboring widths instead: the difference asks what happens when we add one more column. Much of the boundary contribution then cancels.

There is one subtlety. Adding black sites need not add clusters. A new connected piece may join two old clusters and lower the count by one. Whether the two old pieces were already connected far away changes this increment. Free and wired boundaries represent the two extremes of that missing information.

Adjoin an extra column of $m$ deterministic black vertices to the left of $B_{m,k}$, with its usual vertical and horizontal edges. Let $e^w(m,k)$ be the expected number of black clusters in this augmented graph, including the cluster of the deterministic column. The superscript $w$ means *wired*: every black component touching the left edge of the random rectangle becomes connected to the same boundary component. There are still $mk$ random sites.

The wired column belongs to the graph; it is not an additional random column. It contributes one cluster even if every random site is white. This convention matters for finite formulas, although a constant term disappears after division by the strip length.

For $k \geq 2$, define the expected increments

$$d_k^f(m) = e(m,k) - e(m,k-1), \qquad d_k^w(m) = e^w(m,k) - e^w(m,k-1).$$

The column being added is always the rightmost one. In a coupled realization, the two terms in each difference use the same coloring on the common old columns. We are taking an expectation of an increment, not comparing two unrelated pictures.

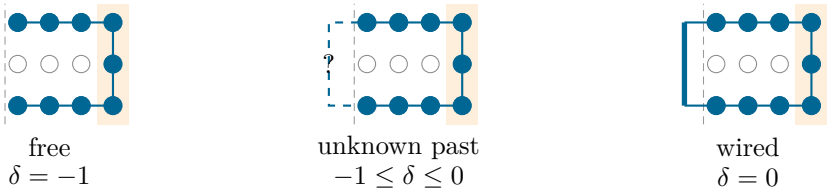



Figure 2: The orange column is new. In the free picture it joins two separate old components. An unseen connection to the left may have already joined them. The wired picture supplies that connection with certainty. The colors in the observed strip are identical in all three pictures; only the old connectivity changes.

### 3.2 A deterministic comparison of connectivity

**Lemma 3.1** (Monotonicity under boundary connections)**.** *Fix the occupied vertices in an old region and in a new column. Adding connections between old components can only increase the increment in the number of components produced by adding the new column.*

*Proof.* We prove a statement about a fixed coloring, before taking any expectations. Let the old graph have $c$ components and the new column have $t$ occupied components. Contract each of these $c+t$ pieces to a vertex. Form a bipartite incidence graph $J$ by joining an old vertex to a new vertex whenever the corresponding pieces are adjacent.

Before adding these incidence edges there are $c+t$ components. Adding them reduces that number by $\operatorname{rank} J = |V(J)| - \#\{\text{components of } J\}$: a spanning tree in each component performs

exactly that many successful mergers. The resulting count is $c + t - \operatorname{rank} J$, whereas the old count was $c$. Thus the increment is

$$\delta = t - \operatorname{rank} J, \qquad \operatorname{rank} J = |V(J)| - \#\{\text{components of } J\}.$$

An additional old connection is represented by identifying two old vertices of $J$. There are exactly two cases.

- If those vertices already belong to the same component of $J$, its number of components stays fixed while its number of vertices drops by one. The rank drops by one, so the increment rises by one.
- If the vertices belong to different components of $J$, both numbers drop by one. The rank, and hence the increment, stays fixed.

Neither operation lowers the increment. Every collection of extra old connections is a sequence of such identifications, proving the lemma. Isolated old components may be included in $J$: each adds one vertex and one component and therefore contributes zero to its rank.

Notice that this proof allows the new column to touch many old components at once. It does not assume that the two cluster counts being compared differ by only zero or one. □

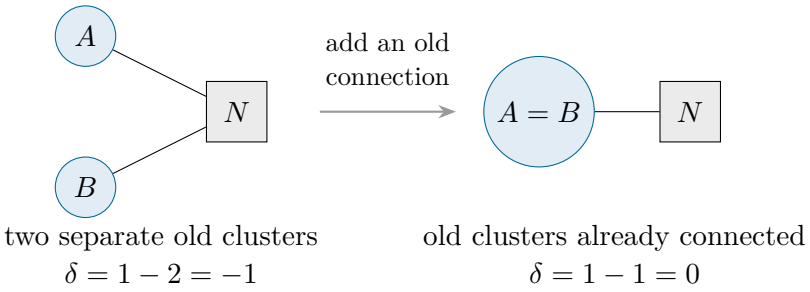



Figure 3: One new occupied component joins two old components. An existing connection between the old components raises the increment.

### 3.3 The finite-strip sandwich

The lemma explains the directions of the two bounds. More old connections mean fewer *new* mergers, and consequently a larger increment. Figure 3 isolates this effect.

**Proposition 3.2** (The finite-strip sandwich)**.** *For every $m \geq 1$ and $n \geq k \geq 2$,*

$$d_k^f(m) \leq e(m,n) - e(m,n-1) \leq d_k^w(m). \tag{3.1}$$

*Moreover $d_k^f(m)$ is nondecreasing in $k \geq 2$, and $d_k^w(m)$ is nonincreasing in $k \geq 2$.*

*Proof.* Fix a coloring of an $m$-by-$n$ rectangle and reveal only its last $k$ columns. The rightmost revealed column is the new one; the preceding $k-1$ columns are the observed old region. Any path through the omitted part must leave and reenter this old region through its left boundary. Thus the

omitted part can only identify some of its boundary-touching components. It cannot create a new adjacency to the rightmost column.

Deleting the omitted part leaves all those extra identifications absent: this is the free increment. Replacing it by one connected black column makes every possible identification among the boundary-touching components: this is the wired increment. The actual equivalence relation lies between these two. Applying Lemma 3.1 gives the inequalities for this coloring. Averaging gives (3.1), since the colors in the revealed strip have the same product law as those in a fresh $m$-by-$k$ rectangle.

Enlarging a free observation window supplies additional old connections and therefore raises its increment. Moving a wired boundary one column farther away replaces maximal connections at the nearer boundary by some subset of those connections, and therefore lowers its increment. These comparisons also hold pointwise under the same coupling. □

### 3.4 From finite rectangles to infinite strips

The next step is a limit argument, not a new connectivity assertion. We spell it out to keep the strip length and strip width distinct. Define the strip rates

$$a_k = \lim_{m\to\infty} \frac{e(m,k)}{m}, \qquad b_k = \lim_{m\to\infty} \frac{e^w(m,k)}{m}. \tag{3.2}$$

Fekete's lemma gives the first limit. For the second, cutting across the length splits the wired column into two pieces, each counted as a cluster in its own rectangle. Rejoining them merges these two components and may merge others. Thus

$$e^w(m_1+m_2,k) - 1 \le (e^w(m_1,k)-1) + (e^w(m_2,k)-1),$$

so Fekete applies again. Both sequences are bounded below by zero after the displayed normalization: $e(m,k) \ge 0$ and $e^w(m,k) - 1 \ge 0$. The rates therefore exist as finite nonnegative numbers.

We also need a precise bridge from these one-dimensional limits to the plane. Fekete's lemma gives

$$a_k = \inf_{m\ge 1} \frac{e(m,k)}{m}.$$

The sequence $a_k$ is subadditive in $k$, by dividing (2.7) by $m$ and taking the limit in $m$. Applying Fekete once more, and then (2.8), gives

$$\lim_{k\to\infty} \frac{a_k}{k} = \inf_{k\ge 1} \frac{a_k}{k} = \inf_{k,m\ge 1} \frac{e(m,k)}{mk} = \lambda. \tag{3.3}$$

This chain of infima justifies the passage between strip rates and the joint limit; an unsupported exchange of limits is unnecessary.

**Theorem 3.3** (Convergent bounds)**.** *For $k \ge 2$, put $L_k = a_k - a_{k-1}$ and $U_k = b_k - b_{k-1}$. Then*

$$L_k \le \lambda \le U_k, \qquad L_k \uparrow \lambda, \quad U_k \downarrow \lambda. \tag{3.4}$$

*Proof. Step 1: turn the finite sandwich into bounds on the density.* Fix $m, k$. Sum (3.1) over $n = k, \dots, N$. The middle terms telescope, giving

$$(N-k+1)d_k^f(m) \le e(m,N) - e(m,k-1) \le (N-k+1)d_k^w(m).$$

Divide by $N$ and send $N$ to infinity. The fixed end term disappears. Since $e(m,N) = e(N,m)$ by rotating a square-grid rectangle, the middle limit is $a_m$. Hence

$$d_k^f(m) \le a_m \le d_k^w(m).$$

Now divide by $m$ and let $m \to \infty$. The left and right limits are $a_k - a_{k-1}$ and $b_k - b_{k-1}$. The middle tends to $\lambda$ by (3.3). This proves $L_k \le \lambda \le U_k$.

*Step 2: check monotonicity and compare the two strip rates.*

The monotonicities follow from Proposition 3.2. If $T$ is the number of black components touching the left edge of a random rectangle, adjoining the wired column changes the cluster count by exactly $1 - T$. Since $0 \le \mathbb{E}T \le m/2$,

$$a_k - \frac{1}{2} \le b_k \le a_k. \tag{3.5}$$

Consequently both $a_k/k$ and $b_k/k$ tend to $\lambda$.

*Step 3: use telescoping averages to identify the endpoints.* Monotonicity and the bounds already proved imply that $L_k$ has a limit $L \le \lambda$, while $U_k$ has a limit $U \ge \lambda$. But

$$\frac{L_2 + \cdots + L_k}{k-1} = \frac{a_k - a_1}{k-1} \longrightarrow \lambda, \qquad \frac{U_2 + \cdots + U_k}{k-1} = \frac{b_k - b_1}{k-1} \longrightarrow \lambda.$$

The averages of a convergent sequence tend to its limit. Their limits must also be $L$ and $U$, so $L = U = \lambda$. This proves both convergence claims, not merely the existence of nested intervals. □

*Remark* 3.4 (Rate of convergence). Only old components connecting the first and penultimate columns can make the free and wired increments differ. Each identification changes the increment by at most one, and each relevant component contains a vertex of the penultimate column. Thus, for $k \ge 3$,

$$0 \le d_k^w(m) - d_k^f(m) \le m\,\mathbb{P}(0 \text{ has an occupied path to distance } k-2).$$

Here the probability on the right is for the full infinite square lattice. Subcritical exponential decay [5] implies $U_k - L_k \le C\exp(-ck)$ for some $c, C > 0$. The convergence proof itself did not need this percolation theorem. Moreover, an unspecified pair $c, C$ is not a numerical error bound. The reported intervals below use the actual computed $L_k, U_k$, with certified arithmetic; they do not substitute an empirical convergence rate into this remark.

### 3.5 Small widths by hand

These examples show what the transfer calculation is remembering. They also give bounds that can be checked without running any code.

**One column.** In width 1, a new black run begins at the first black site or whenever a black site follows a white one. The first site starts a run with probability $1/2$; each of the other $m-1$ sites starts one with probability $1/4$. Hence $e(m,1) = 1/2 + (m-1)/4 = (m+1)/4$ and $a_1 = 1/4$.

**Two columns.** Every nonempty row is connected, so its two colors contain all the necessary boundary information. Here is the complete increment table; 1 denotes black and 0 denotes white.

| old row \ new row | 00 | 10 | 01 | 11 |
|---|---|---|---|---|
| 00 | 0 | 1 | 1 | 1 |
| 10 | 0 | 0 | 1 | 0 |
| 01 | 0 | 1 | 0 | 0 |
| 11 | 0 | 0 | 0 | 0 |

The entries sum to 5. Consecutive random rows have each of the 16 color pairs with probability 1/16, so the expected increment after the first row is 5/16. The first row has a cluster unless it is 00, which gives initial expectation 3/4. Therefore

$$e(m,2) = \frac{5m+7}{16}, \qquad a_2 = \frac{5}{16}.$$

**Three columns and one bit of memory.** In width 3, the only row pattern with an ambiguous connectivity state is black–white–black. Let $h_m$ be the probability that this is the last row and its two black sites are connected through the preceding rows. The first row has $h_1 = 0$, and

$$h_{m+1} = \frac{1}{8}\left(\frac{1}{8} + h_m\right), \qquad h_m = \frac{1}{56}(1 - 8^{1-m}).$$

Indeed, a new black–white–black row has probability 1/8, and its endpoints connect exactly when the previous endpoints were connected: the previous row was either all black, or in the connected ambiguous state. Enumerating the eight new row patterns gives expected increment $3/8 + h_m/8$. For completeness, the mean reward conditional on a frontier state is as follows. Each mean averages the eight possible new rows.

| Old row and its connectivity | Conditional mean increment |
|---|---|
| 000 | 1 |
| 100, 010, or 001 | 1/2 |
| 110 or 011 | 1/4 |
| 111 | 0 |
| 101 with separate ends | 0 |
| 101 with connected ends | 1/8 |

The old row's eight color patterns remain uniform; only the split of 101 between its two connectivity states depends on the past. The first five rows of this table give the baseline 3/8, and the connected state contributes the extra $h_m/8$.

Starting from $e(1,3) = 1$, we therefore have

$$e(m,3) = 1 + \sum_{j=1}^{m-1}\left(\frac{3}{8} + \frac{h_j}{8}\right).$$

Substitute $h_j = (1 - 8^{1-j})/56$ and sum the geometric progression. This gives

$$e(m,3) = \frac{1183m + 1945 + 8^{2-m}}{3136}, \qquad a_3 = \frac{169}{448}. \tag{3.6}$$

**Two random columns beside a wire.** For one random column beside a wired boundary, the graph always has one black cluster, so $b_1 = 0$. For two random columns, let $g_m$ be the probability that the near site in the last row is white, the far site is black, and the latter is connected to the wire through earlier rows. Then

$$g_1 = 0, \qquad g_{m+1} = \frac{1}{4}\left(\frac{1}{4} + g_m\right).$$

To see the recurrence, a new near-white/far-black row has probability $1/4$. Its far site reaches the wire through the previous row exactly when both previous random sites were black (probability $1/4$), or when the previous row was already in the special state (probability $g_m$). These possibilities are disjoint. The recurrence solves to $g_m = (1 - 4^{1-m})/12$.

The expected increment is $1/16 + g_m/4$, by the same finite averaging as above, and the first row has expectation $5/4$. Therefore

$$e^w(m, 2) = \frac{5}{4} + \sum_{j=1}^{m-1}\left(\frac{1}{16} + \frac{g_j}{4}\right) = \frac{3m + 41 + 4^{1-m}}{36}, \qquad b_2 = \frac{1}{12}.$$

In particular Theorem 3.3 recovers the original analytic bounds

$$\frac{29}{448} = a_3 - a_2 \le \lambda \le b_2 - b_1 = \frac{1}{12}. \tag{3.7}$$

The lower and upper bounds in this particular display use different widths.

# 4 Finite-state computation and certification

## 4.1 Remember the frontier, not the whole past

The width-3 example suggests the general method. The newest row is a separator: every path from a future site to an older site must pass through it. We therefore need to know which newest-row sites are black and which of them the past has already connected. We do not need the individual shapes or sizes of components behind the row.




Figure 4: Identical colors on the newest row, different information from the past. The two black endpoints may be separate or connected. If the next row is all black, the left configuration loses one cluster and the right configuration does not. A state records precisely this connectivity.

For a strip of fixed width, record the occupied sites in the newest row, together with the partition specifying which of those sites are connected through the part already exposed. Closed components no longer touching the row cannot affect future connectivity. Labels are canonicalized from left to

right, with zero for a vacant site. For example, $(1, 0, 2)$ and $(1, 0, 1)$ distinguish the two ambiguous width-3 states above.

To process a new row, adjoin its occupied vertices, join adjacent new vertices and the vertical occupied pairs, and identify vertices belonging to the same previous component. The change in cluster count is the number of new occupied vertices minus the number of successful component mergers. Retain only the induced connectivity on the new row. For a wired strip, keep one additional deterministic black position at the left of every row. Its component persists throughout the scan.

There are finitely many such states at fixed width: only finitely many subsets of row sites and partitions of each subset. Starting at the empty frontier (or just the permanent wire), one may discover the reachable states by repeatedly applying all row patterns. The complete past affects the future only through the recorded state, so this constructs a finite Markov chain with transition matrix $P$. It is a standard connectivity-state transfer construction; related finite-automaton formulations appear in [8, 9]. If there are $k$ random sites per row, let $D = 2^k$, so $P = K/D$ for an integer transition-count matrix $K$. Let $r_i$ be the sum of the cluster increments over the $D$ new row patterns from state $i$.

### 4.2 Why the stationary reward is the strip rate

The all-white random row, of probability $1/D$, sends every state to the same reset state. In the wired case the deterministic boundary position remains black. Couple two scans by giving them the same future rows, however different their starting states. Once an all-white random row appears, their states agree and remain equal. The probability that no such row has appeared after $t$ steps is $(1 - 1/D)^t$. Hence the two state distributions become arbitrarily close. A finite chain has a stationary distribution, and this coupling proves that it is unique and attracts every starting law. Write that law as $\pi$.

If $X_t$ is the frontier after $t$ rows, the expected increment at the next row is $\mathbb{E}[r_{X_t}/D]$. Consequently

$$e(m, k) = e(0, k) + \sum_{t=0}^{m-1} \mathbb{E}\left[\frac{r_{X_t}}{D}\right],$$

with the analogous formula for a wire and with its initial count equal to one. Each summand tends to $\sum_i \pi_i r_i/D$. Dividing by $m$ and using convergence of averages proves that the strip rate is

$$a_k = \sum_i \pi_i \frac{r_i}{D} \quad \text{or} \quad b_k = \sum_i \pi_i \frac{r_i}{D}, \tag{4.1}$$

using the corresponding free or wired chain. This follows by summing the expected increments and applying Cesàro convergence. Initial cluster counts disappear after division by length.

### 4.3 An efficient factorization, one site at a time

A literal row update tries all $2^k$ new row patterns from every state. We can factor that same operation into $k$ updates with only two choices each: expose the new row from left to right. At an intermediate stage, the frontier consists of the already exposed part of the new row and the still-unreplaced part of the old row.

If the new site is black, start its reward at 1. Subtract 1 when it joins the old site above or below it, if that site is black. Subtract another 1 if it joins the previously exposed neighbor on its




the next site sees its left neighbor
and the old site in its own column

Figure 5: The frontier moves one site at a time. The next site, circled in orange, has only two neighbors in the exposed graph. Its increment is 0 if vacant; if occupied it is one minus the number of successful mergers with those two neighbors.

left and that neighbor is still a different component. The possible rewards are $-1, 0, 1$. If the new site is white its reward is zero. Remove the old site from the frontier while retaining the equivalence relation it has induced on the remaining sites.

For wired strips we can keep the boundary component permanently present, without representing its vertices row by row. The first random site in each new row has this component as its left neighbor. The resulting random row still has $k$ coin flips and the same cluster-count increment. The product of the $k$ two-choice transition operators is exactly $P$. Accumulating the site rewards gives exactly the row reward. This changes the cost of the computation, not the quantity being bounded.

Planarity allows an additional storage saving. Along the frontier, connected blocks are noncrossing: two blocks cannot alternate in the order $A, B, A, B$, since disjoint paths through the exposed planar region would then have to cross. A block can be encoded by marking its first, intermediate, and last positions; singletons and vacant positions have their own marks. The code enumerates noncrossing partitions consistent with already-present edges, checks that every transition stays within these lists, and checks the common reset from every row state. It does not require a claim that every enumerated state is reachable. Extra transient states do not affect the unique law reached from the reset.

### 4.4 Turn an approximate stationary vector into a proof

Small chains can be solved over the rational numbers. Larger chains are handled by approximate stationary vectors followed by exact residual certification. The latter step is essential for an enclosure.

**Proposition 4.1** (Integer residual certificate)**.** *Choose integers $q_i \geq 0$ with $\sum_i q_i = Q$, and define*

$$R = \sum_j \left| \sum_i q_i K_{ij} - D q_j \right|, \qquad \widehat{a} = \frac{\sum_i q_i r_i}{QD}.$$

*If $|r_i/D| \leq w$ for every state, the stationary mean reward lies in*

$$\left[ \widehat{a} - \frac{wR}{Q}, \, \widehat{a} + \frac{wR}{Q} \right]. \tag{4.2}$$

*The site-by-site update shows that one may take $w = k$ for both models.*

*Proof.* Write $\delta = 1/D$. Because every row of $P$ assigns mass at least $\delta$ to the same reset state,

$$P = \delta J + (1 - \delta) S,$$

where every row of $J$ is the point mass at that state and $S$ is a stochastic matrix. If a signed row vector $\eta$ has total mass zero, then $\eta J = 0$. Also $\|\eta S\|_1 \le \|\eta\|_1$, by the triangle inequality and the row sums of $S$. Therefore

$$\|\eta P\|_1 \le (1-\delta)\|\eta\|_1.$$

This is the quantitative version of the reset coupling.

Normalize the proposed integer masses to $v = q/Q$. It is an actual probability vector because all $q_i$ are nonnegative and sum to $Q$. Compare it with the true stationary law, using $\pi P = \pi$:

$$\|v-\pi\|_1 \le \|vP - \pi P\|_1 + \|v - vP\|_1 \le (1 - 1/D)\|v-\pi\|_1 + \|v - vP\|_1.$$

Therefore $\|v-\pi\|_1 \le D\|v - vP\|_1 = R/Q$. The exact residual is

$$\|vP - v\|_1 = \frac{1}{QD}\sum_j \left|\sum_i q_i K_{ij} - Dq_j\right| = \frac{R}{QD}.$$

Finally, if $g_i = r_i/D$ and $|g_i| \le w$, then

$$|\pi g - vg| \le \sum_i |\pi_i - v_i|\,|g_i| \le w\|\pi - v\|_1 \le \frac{wR}{Q}.$$

Since $vg = \widehat{a}$, this is precisely (4.2). The argument does not assume that the floating-point iteration converged to any specified tolerance. It certifies whichever nonnegative integer vector was actually supplied. □

### 4.5 Certified intervals and what they improve

The original whole-row implementation uses $Q = 2^{60}$; the factored implementation uses $Q = 2^{80}$. In the latter, each of the $k$ random site updates has absolute reward at most one, so $w = k$ is valid for both boundary conditions. Floating arithmetic is used to find a good candidate $q$; all masses, residuals, interval endpoints, and outward decimal rounding are then treated exactly. Differences of consecutive intervals give Table 1. Exact rational solves through width 7 independently check these intervals. For the wider strips, the factored implementation also agrees with the separate whole-row implementation on every width computed by both. Every possible row update through width 8 was checked against the whole-row union-find rule, including its reward.

Suppose a free rate has certificate $[a_k^-, a_k^+]$, and a wired rate has certificate $[b_k^-, b_k^+]$. The guaranteed bounds are

$$a_k^- - a_{k-1}^+ \le \lambda \le b_k^+ - b_{k-1}^-.$$

The signs matter: subtracting approximate central values without their errors would not give a rigorous enclosure. Decimal lower endpoints are rounded downward and upper endpoints upward.

**Corollary 4.2** (Computed enclosure)**.** *The transfer calculation and Proposition 4.1 give*

$$\boxed{0.06576983 \le \lambda \le 0.06577780.}$$

The displayed interval has width

$$0.06577780 - 0.06576983 = 0.00000797 < 8 \cdot 10^{-6}.$$

| Width $k$ | Lower bound for $\lambda$ | Upper bound for $\lambda$ |
|---|---|---|
| 2 | 1/16 | 1/12 |
| 3 | 0.0647321428 | 0.0722323601 |
| 4 | 0.0653516433 | 0.0688155384 |
| 5 | 0.0655783692 | 0.0673756711 |
| 6 | 0.0656748763 | 0.0666765674 |
| 7 | 0.0657200802 | 0.0663059641 |
| 8 | 0.0657427144 | 0.0660975054 |
| 9 | 0.0657546225 | 0.0659751478 |
| 10 | 0.0657611316 | 0.0659010006 |
| 11 | 0.0657647996 | 0.0658549480 |
| 12 | 0.0657669185 | 0.0658257819 |
| 13 | 0.0657681681 | 0.0658070179 |
| 14 | 0.0657689179 | 0.0657947894 |
| 15 | 0.0657693746 | 0.0657867343 |
| 16 | 0.0657696564 | 0.0657813803 |
| 17 | 0.0657698321 | 0.0657777945 |

Table 1: Free/wired strip bounds. All displayed decimals are rounded outward. The bounds at width 2 are exact fractions.

Thus this computation gives a window on the scale of $10^{-6}$. The initial repaired draft, using width 10, gave $[0.06576113, 0.06590101]$, of width 0.00013988. The present enclosure is about 17.5 times narrower. At width 17 the free and wired row chains have 6,536,382 and 11,662,902 states, respectively.

The arithmetic errors in the four rates used for the final interval are each below $3 \cdot 10^{-10}$. Those small arithmetic errors must not be confused with the larger error due to finite strip width. In particular, we have not certified a $10^{-10}$-wide window for $\lambda$. No numerical extrapolation of the strip sequence is used in the bound.

**Comparison with previous work.** The new interval improves both the valid analytic bounds of the thesis and the first repaired draft's computed enclosure. Published numerical estimates are more precise: Ziff, Finch and Adamchik give the Monte Carlo estimate $0.0657703 \pm 0.0000002$ and the series-based estimate 0.0657696(6) [2]. These uncertainties are not deterministic interval certificates. The small-width enumerations in [8, 9] concern finite strips, while the general density and boundary arguments are classical [7]. The sources reviewed here do not establish the best published rigorous numerical enclosure at $p = 1/2$. We therefore make no record or priority claim for the displayed interval.

This is a computer-assisted result: the comparison theorem is proved above, and its finite numerical inputs are certified by integer arithmetic. The code regenerates and checks those certificates. The calculation has not been formalized in a proof assistant. It also rules out the lower bound 0.067105 printed in the original thesis. The original program was unavailable, so no diagnosis of its particular error is asserted.

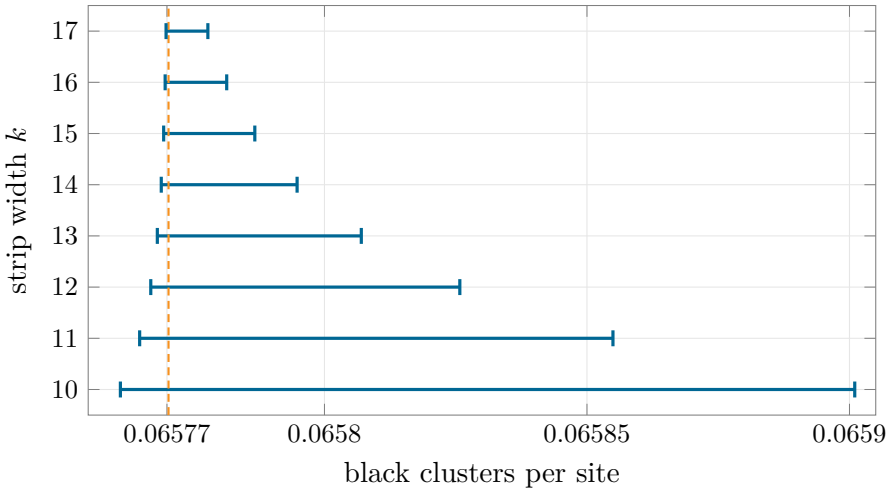



Figure 6: Certified strip intervals narrow as more columns are retained. The dashed line is the published numerical estimate 0.0657703, shown for comparison; it plays no role in certifying any endpoint.

# 5 An Euler identity and cluster expansions

## 5.1 Counting components by counting holes

There is a second description of $\lambda$ that explains the conspicuous number $1/16$ in elementary lower bounds. In the plane, a graph's number of components is related to its numbers of vertices, edges, and holes. The local counts of vertices and edges are particularly easy to average. To identify the holes correctly for site percolation, we must also keep track of all-black unit squares and of diagonal connections between white sites.

Let the *matching graph* of the square lattice have all eight nearest horizontal, vertical, and diagonal neighbors. We also call it the king's graph. Write $n_*(p)$ for its density of finite black clusters at occupation probability $p$. Infinite clusters contribute zero to this density, as in Theorem 2.1.

**Theorem 5.1** (Square-lattice matching identity)**.** *For* $0 \le p \le 1$*,*

$$n_{\square}(p) - n_*(1-p) = p - 2p^2 + p^4. \tag{5.1}$$

*In particular,*

$$\lambda = \frac{1}{16} + n_*(1/2). \tag{5.2}$$

*Proof. Step 1: draw the black graph and fill its all-black unit faces.* In a finite rectangle, draw all black vertices and all nearest-neighbor edges whose endpoints are black. Let their counts be $V_{\text{black}}$ and $E_{\text{black}}$. This planar graph has $K^{\text{black}}$ connected components. Euler's formula says that the number of bounded components of its complement is $E_{\text{black}} - V_{\text{black}} + K^{\text{black}}$.

Some of those complementary components are simply unit squares with four black corners. There is no white vertex inside such a square, so it should not represent a white cluster. Fill every such unit square with a face; denote their number by $F_{\text{black}}$. Each filling removes exactly one bounded complementary component without changing the black connected components. The number $H$ of

holes remaining is therefore

$$H = E_{\text{black}} - V_{\text{black}} + K^{\text{black}} - F_{\text{black}}.$$

*Step 2: identify the remaining holes with white matching clusters.* Every unfilled unit face has at least one white corner. Within its interior, any of its white corners can be joined while avoiding the black graph. Adjacent unit faces communicate through a white corner or an edge not occupied by the black graph. Thus following a path through the complement amounts to following horizontal, vertical, or diagonal steps between white lattice sites. Conversely, each such white step can be drawn in the complement. This gives the king's-graph adjacency, rather than just nearest-neighbor white adjacency.

The unbounded complementary component contains exactly the white king's-graph components that meet the rectangle's boundary. The bounded components contain exactly those that do not meet it. Writing the number of the latter as $H_*^{\text{white}}$, we have $H = H_*^{\text{white}}$ and hence

$$K^{\text{black}} - H_*^{\text{white}} = V_{\text{black}} - E_{\text{black}} + F_{\text{black}}. \tag{5.3}$$

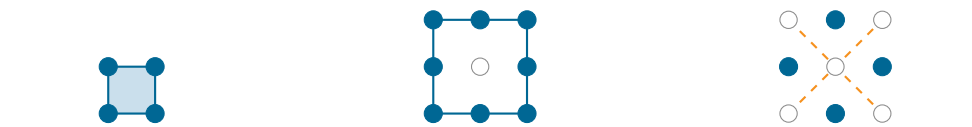
Figure 7 illustrates why both the filling rule and the white diagonal edges are necessary.

*Step 3: average the local counts and discard the boundary.* There are $mn$ vertices, $2mn - m - n$ nearest-neighbor edges, and $(m-1)(n-1)$ unit faces. By independence of the colors at their endpoints or corners,

$$\mathbb{E}V_{\text{black}} = mnp, \qquad \mathbb{E}E_{\text{black}} = (2mn - m - n)p^2, \qquad \mathbb{E}F_{\text{black}} = (m-1)(n-1)p^4.$$

These formulas use linearity of expectation; different edges or faces do not need to be independent of one another.

The difference between $H_*^{\text{white}}$ and the total number of white king's-graph clusters is at most the number of boundary vertices, since each omitted component contains one of those vertices. After division by $mn$, its expected contribution vanishes as both sides grow. Theorem 2.1 applies to both adjacency rules. Dividing (5.3) by $mn$ and passing to expectations and limits gives $n_{\square}(p) - n_*(1-p) = p - 2p^2 + p^4$. Substitution of $p = 1/2$ gives $\lambda = 1/16 + n_*(1/2)$. □



$V = 4,\ E = 4,\ F = 1$
$K = 1,\ H = 0$

$V = 8,\ E = 8,\ F = 0$
$K = 1,\ H = 1$

white center escapes
through diagonal steps

Figure 7: Three local checks on the Euler argument. Left: fill an all-black unit square so that its empty interior is not counted as a white cluster. Middle: a black ring surrounds one genuine white hole. Right: four isolated black sites do not enclose a hole; the white center connects to the boundary by king's moves.

### 5.2 The Putnam bound, and a better bound from three shapes

This is the square-lattice case of the Sykes–Essam matching relation; see [4, 3]. The proof above also directly answers the finite Putnam question. At $p = 1/2$, the expectation of the right side of (5.3) is

$$\frac{mn}{2} - \frac{2mn - m - n}{4} + \frac{(m-1)(n-1)}{16} = \frac{mn + 3m + 3n + 1}{16}.$$

Since $H_*^{\text{white}} \geq 0$, the expected number of regions of both colors is at least $(mn + 3m + 3n + 1)/8 > mn/8$.

**Corollary 5.2** (A short stronger lower bound)**.**

$$\lambda \geq \frac{533}{8192} = 0.0650634765625.$$

*Proof.* An isolated occupied king's-graph site has eight vacant neighbors, so its contribution is $2^{-9} = 1/512$. For a horizontal or vertical adjacent pair, there are ten distinct outside neighbors; the two orientations contribute $2 \cdot 2^{-12}$. For a diagonal pair there are twelve outside neighbors; its two orientations contribute $2 \cdot 2^{-14}$. Thus the two-site contribution is $5/8192$. Keeping only these nonnegative terms in (5.2) gives

$$\lambda \geq \frac{1}{16} + \frac{1}{512} + \frac{5}{8192}.$$

□

The bound in Corollary 5.2 is stronger than $29/448$ and needs only three small shapes. It does not evaluate $\lambda$ in closed form: the remaining king's-graph density is itself a nontrivial constant. We know no elementary closed form for the square-site density at $1/2$.

### 5.3 Polyomino sums with an explicit remainder

Let $\mathcal{A}_s$ be the translation classes of nearest-neighbor connected sets of $s$ sites. Rotations and reflections are kept as distinct classes when they give different sets up to translation. For a representative $A$, let $\partial A$ be its set of distinct outside nearest neighbors. To obtain a cluster exactly equal to a specified translate of $A$, every site in $A$ must be black and every site in $\partial A$ must be white. There is no restriction on any other site. Independence therefore gives probability $2^{-|A|-|\partial A|}$.

Choose the lexicographically first site as the anchor of a shape. There is exactly one possible anchor per lattice site and one anchored orientation per translation class. Summing the probabilities that the origin anchors each possible cluster counts each cluster once, so

$$n_s = \sum_{A \in \mathcal{A}_s} 2^{-s-|\partial A|}, \qquad \lambda = \sum_{s \geq 1} n_s. \tag{5.4}$$

One can equally sum over free polyominoes if each is weighted by its number of distinct orientations. The boundary counts vertices, not edges. In particular, an outside site adjacent to two sites of the shape is still only one required white site. This distinction is visible in Figure 8.

Because all occupied square-site clusters are finite at $p = 1/2$, $\sum_s s n_s = 1/2$. After retaining sizes at most $N$, the omitted occupied-site mass is $R_N = 1/2 - \sum_{s \leq N} s n_s$. Each omitted cluster uses at least $N + 1$ sites, so its density is at most $R_N/(N+1)$:

$$\sum_{s > N} n_s \leq \frac{1}{N+1} \sum_{s > N} s n_s = \frac{R_N}{N+1}.$$



straight triomino
$|\partial A| = 8$, probability $2^{-11}$

bent triomino
$|\partial A| = 7$, probability $2^{-10}$

Figure 8: Exterior vertex boundaries of the two triomino shapes. The circled white site touches two occupied sites but is counted only once. There are two orientations of the straight shape and four of the bent shape, giving $n_3 = 2 \cdot 2^{-11} + 4 \cdot 2^{-10} = 5/1024$.

This gives the rigorous enclosure

$$\sum_{s \le N} n_s \le \lambda \le \sum_{s \le N} n_s + \frac{1/2 - \sum_{s \le N} s n_s}{N+1}. \tag{5.5}$$

This controls the tail without importing a numerical percolation estimate. The upper bound remains valid if an infinite cluster is allowed, since using $1/2$ then only overestimates the remaining finite-cluster mass.

| Size $s$ | Translation classes | Contribution $n_s$ |
|---|---|---|
| 1 | 1 | 1/32 |
| 2 | 2 | 1/128 |
| 3 | 6 | 5/1024 |
| 4 | 19 | 27/8192 |
| 5 | 63 | 157/65536 |
| 6 | 216 | 953/524288 |
| 7 | 760 | 6029/4194304 |
| 8 | 2725 | 39273/33554432 |

Table 2: Exact square-polyomino contributions from independent enumeration.

The sum through size 8 is

$$\frac{1814033}{33554432} = 0.05406239628791809\ldots.$$

The corresponding upper bound in (5.5) is less than 0.09661608604, so this small cutoff is not competitive with the strip bounds. Exponential cluster-size tails make larger cutoffs effective in principle, but the number of shapes grows exponentially.

As a simpler example, the sum over rectangles alone is

$$\sum_{i \ge 1} \sum_{j \ge i} \frac{2 - \mathbf{1}_{\{i=j\}}}{2^{ij+2i+2j}} = 0.04045577197\ldots.$$

A square has one orientation, whereas a nonsquare rectangle has two. Analogous enumeration on the king's graph through size 6, added to $1/16$, gives $0.06560994416940957\ldots$ as a lower bound.

# 6 Boundary conditions and cycles

## 6.1 A torus has the same bulk density

Let $e_T(m,n)$ be the expected black-cluster count after adding periodic edges in both directions, disregarding duplicate edges and self-loops. There are at most $m+n$ additional edges. Each decreases the cluster count by at most one and can do so only when both endpoints are occupied. Therefore

$$0 \le e(m,n) - e_T(m,n) \le \frac{m+n}{4}, \tag{6.1}$$

After division by $mn$, the upper bound is $\frac{1}{4}(1/m+1/n)$, which tends to zero when both side lengths tend to infinity. This proves equality of the full two-dimensional densities. It also shows precisely why the argument does not apply when one side length is fixed.

For a strip of fixed width, the transverse periodic edges occur all along its length. There is one possible seam edge per row, so their number is proportional to the length rather than confined to two end rows. They cannot be discarded as a vanishing boundary term.



free width-3 strip
each row is a path

periodic across the width
one extra edge per row

Figure 9: Underlying graphs before coloring. Across a width-3 cylinder, the first and last sites of every row are adjacent, so every nonempty occupied row is connected. The orange seam occurs throughout the strip.

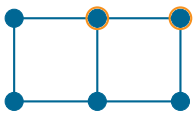
For example, the three sites in a transverse row of a width-3 cylinder form a triangle, so every nonempty row is connected. A new row contributes one component exactly when it is nonempty and disjoint from the occupied sites of the previous row. To count this event, fix the nonempty set $A$ of black sites in the new row. The previous occupied set can be any subset of its complement, giving $2^{3-|A|}$ possibilities. The $8^2$ ordered pairs of rows are equally likely. Thus its stationary mean increment is

$$\frac{1}{8^2} \sum_{\varnothing \neq A \subseteq \{1,2,3\}} 2^{3-|A|} = \frac{3^3 - 2^3}{64} = \frac{19}{64}.$$

Closing the long direction changes the count by at most three. Thus the width-3 torus-strip rate is 19/64, different from the free rate 169/448 in (3.6).

## 6.2 The scan loops count cycle rank

Scan a square rectangle row by row, from left to right. A black vertex closes a loop when its left and lower neighbors are both black and already connected in the previously exposed graph. Let $X_{m,n}$ count these events. They count the number of independent cycles, rather than every simple cycle in the graph. For example, the two adjacent squares in Figure 10 have three simple cycles, but only two independent ones: over the two-element field, the outer boundary is the sum of the two square boundaries.



$V = 6, \quad E = 7, \quad K = 1$
$\beta_1 = E - V + K = 2$
three simple cycles

Figure 10: Scan the bottom row first, then the top row from left to right. The two circled vertices each close one independent cycle. No two-dimensional faces are filled in this graph calculation; it is the cycle rank before the face correction used in Section 5.

**Proposition 6.1.**

$$\mathbb{E}X_{m,n} = e(m,n) - \frac{m+n}{4}.$$

*Proof.* For any occupied induced graph, its cycle rank is $\beta_1 = E_{\text{black}} - V_{\text{black}} + K_{\text{black}}$. A scanned black vertex has $q \in \{0,1,2\}$ black neighbors in the already exposed graph. Suppose these neighbors belong to $c$ distinct old components. Adding the vertex changes the counts by

$$\Delta V = 1, \qquad \Delta E = q, \qquad \Delta K = 1 - c.$$

Consequently $\Delta\beta_1 = q - c$. The possible cases are

| Old neighbors | $q$ | $c$ | $\Delta K$ | $\Delta\beta_1$ |
|---|---|---|---|---|
| none | 0 | 0 | 1 | 0 |
| one | 1 | 1 | 0 | 0 |
| two, in different components | 2 | 2 | $-1$ | 0 |
| two, already connected | 2 | 1 | 0 | 1 |

A white site changes none of these counts. Thus the cycle rank rises exactly at the loop-closing events defining $X_{m,n}$, and starts at zero. This proves $X_{m,n} = \beta_1$ for every coloring. Taking expectations,

$$\mathbb{E}X_{m,n} = \frac{2mn - m - n}{4} - \frac{mn}{2} + e(m,n).$$

□

As a small check, a 1-by-$m$ graph has no cycles. Its formula $e(m,1) = (m+1)/4$ makes the right side of Proposition 6.1 zero, as it should. An erroneous constant in that identity would already fail this one-dimensional check.

In particular $\mathbb{E}X_{m,n}/(mn) \to \lambda$. Equivalently, the occupied graph has the same asymptotic cycle-rank density as its component density at probability one half.

### 6.3 The triangular variant

Adding the edges $(x,y) \sim (x+1, y+1)$ gives the degree-6 triangular lattice, also represented by adjacency of hexagonal cells. It is not the degree-3 honeycomb graph. Let $e_\triangle$ and $\lambda_\triangle$ denote its corresponding counts and density.

The reciprocal-size proof, finite-state construction, and free/wired comparison work with these extra edges. Swapping the two coordinates preserves this particular diagonal convention, so the

same telescoping argument gives bounds for $\lambda_\triangle$. The formulas in Appendix A give

$$\frac{1}{112} \le \lambda_\triangle \le \frac{1}{24}.$$

The model is critical at probability one half; the exponential convergence argument for the subcritical square model should not be imported here. For comparison, the numerical series estimate reported in [3] is 0.017625277368(2).

The boundary of a triangular-lattice cluster need not be one entire opposite-colored cluster: a black annulus can have separate white components inside and outside. We therefore make no identification of the number of boundary clusters with the scan statistic above.

## 7 Reproducibility and the status of this draft

The accompanying code has three implementations of strip transfers: Python with exact rational linear algebra, a C++ whole-row transfer, and a C++ transfer factored into single-site updates. Both C++ versions certify their stationary rewards by exact integer residuals. Separate routines count components by flood fill on small finite colorings. The checks include:

- exact stationary equations, nonnegativity, and normalization for free and wired square strips through width 7;
- agreement of the numerical certificates with every available exact strip rate, and certified interval subtraction through width 17;
- agreement with the independent whole-row calculation through width 12, and exhaustive checks of all row transitions through width 8;
- direct enumeration through 3 by 3 random rectangles for square and triangular adjacency, with both boundary conditions;
- the finite Euler identity on all 74,954 colorings of rectangles with each dimension from 1 through 4, and 12,288 pointwise increment sandwiches on 3 by 4 colorings;
- exact recurrence certificates for all the small-width formulas in Appendix A, valid for every positive length;
- complete exterior vertex-boundary histograms for square animals through size 9 and king's-graph animals through size 6.

These checks have distinct roles. Finite enumeration checks the graph rules; stationary equations and residual bounds certify the strip calculation; the mathematical comparison theorem turns those strip rates into bounds on the infinite-volume constant.

For a direct check of the displayed final enclosure, run

```
python3 code/verify_enclosure.py
```

This compiles the factored transfer in a temporary directory, recomputes the four strip rates needed for the last pair of bounds, certifies them by integer arithmetic, and checks that the resulting interval

is contained in the one stated here. It requires Python 3 and a C++17 compiler supporting 128-bit integers. The largest computation needs several gigabytes of memory and can take many minutes.

The full width table can be regenerated with

```
python3 code/certify_layers.py --max-width 17
```

An optional output directory retains the full integer candidate vectors; a separate verification mode reads those vectors and performs no floating-point iteration. Compact result summaries accompany the paper. The large candidate vectors can be regenerated when needed rather than being included in every copy of the paper download.

The public-facing byline "Jacob Richey + ChatGPT" records how this draft was made. It does not transfer the 2014 thesis to a new author or claim that an AI review constitutes final verification. The replacement proofs and code remain available for inspection, and this version is labeled as a working draft pending Jacob's full review.

# A Corrected finite-strip formulas

Here $m \geq 1$ is the length and $k$ the number of random columns. For either adjacency, a single wired random column gives expectation 1. The corrected square formulas are

$$e(m,1) = \frac{m+1}{4}, \qquad e(m,2) = \frac{5m+7}{16},$$
$$e(m,3) = \frac{1183m + 1945 + 8^{2-m}}{3136}, \qquad e^w(m,2) = \frac{3m + 41 + 4^{1-m}}{36}.$$

For the triangular lattice,

$$e_\triangle(m,1) = \frac{m+1}{4}, \qquad e_\triangle(m,2) = \frac{m+2}{4},$$
$$e_\triangle(m,3) = \frac{203m + 573 + 8^{2-m}}{784}, \qquad e^w_\triangle(m,2) = \frac{3m + 83 + 4^{2-m}}{72}.$$

The square formulas were derived in Section 3. All formulas, including the triangular ones, also have exact recurrence certificates. For completeness, here is the finite-dimensional argument that makes such a certificate valid for every length. If $P$ is a strip's transition matrix and $r$ its column vector of mean rewards, use the augmented matrix

$$T = \begin{pmatrix} P & r \\ 0 & 1 \end{pmatrix}.$$

Write the augmented row vector as $z_m = (\mu_m, e_m)$, where $\mu_m$ is the frontier distribution and $e_m$ is the accumulated expected cluster count. Matrix multiplication gives

$$z_m T = (\mu_m P,\ e_m + \mu_m r).$$

This is exactly one transfer step: update the distribution and add its mean reward. Starting with unit mass at the reset state and count 0 (free) or 1 (wired), the last coordinate of $z_0 T^m$ is therefore the expected cluster count after $m$ rows. For an affine formula use $A(t) = (t-1)^2$; for a formula with an additional $q^{m-1}$ term, use $A(t) = (t-1)^2(t-q)$, where $q = 1/8$ or $1/4$ above.

Writing $v$ for the last-coordinate vector and $d = \dim T$, the program verifies exactly that

$$z_0 T^j A(T) v = 0 \quad (1 \le j \le d).$$

Here is why finitely many zero residuals suffice. By Cayley–Hamilton, $T^d$ is a linear combination of $I, T, \dots, T^{d-1}$. Multiply that identity by $z_0 T$ on the left and $A(T)v$ on the right: the next residual is a linear combination of the first $d$, hence is zero. Repeating proves that every residual with $j \ge 1$ is zero.

Writing $A(t) = \sum_{i=0}^{\ell} c_i t^i$, with $c_\ell = 1$, the vanishing residual is the recurrence $\sum_{i=0}^{\ell} c_i e_{j+i} = 0$. The proposed closed form obeys this recurrence too: two differences kill its affine part, and the extra factor $t - q$ kills its geometric part. Checking the first $\ell = \deg A$ positive-length values now identifies the two sequences for every $m \ge 1$. This is a proof of the entire formula. This proves more than checking a finite list of numerical examples. The rational recurrence certificates and initial values are supplied with the data.

## B Relation to the 2014 thesis

This draft preserves the problem and the free/wired increment method, but reorganizes the exposition around proofs that can be checked independently. The following changes are the substantive ones; page numbers refer to the printed pages of the original thesis.

1. The density proof on pages 10–11 is replaced by the reciprocal identity and rectangular subadditivity. The unnormalized asymptotic error asserted there is removed.

2. The mean-size discussion on pages 4 and 14–15 is replaced by (2.6). The proposed self-avoiding-walk identity is removed.

3. The page-14 discussion of infinite clusters is corrected. Square-site probability one half is subcritical, and square-site critical percolation has no infinite cluster [6].

4. The full torus-density equality is retained. The false fixed-width equality in Corollary 3.2 is replaced by the explicit width-3 counterexample in Section 6.

5. Proposition 3.3's comparison is retained, with a connectivity-rank proof. Its passage to limiting densities is justified by telescoping, and monotone convergence of the bounds is proved.

6. The loop formula on pages 20–21 loses the erroneous additive 1/2. The triangular boundary-cluster interpretation is not used.

7. The finite-strip table is corrected for its factors of two, variable, exponent, and sign errors. The size-7 and size-8 polyomino coefficients are replaced by Table 2.

8. The page-23 interval $[0.067105, 0.0677055]$ is withdrawn and replaced by Corollary 4.2. No original computational files were available to identify how that interval arose.

The matching-lattice treatment and the complete computational certification are part of this revision. The matching relation itself is classical, and the constant had been numerically studied well before 2014. No novelty claim is made for the general transfer-matrix framework or for the standard percolation identities.

## References


[1] J. Richey, *Counting Clusters on a Grid*, undergraduate honors thesis, Dartmouth College, 2014. Advisor: P. Winkler. Original thesis.

[2] R. M. Ziff, S. R. Finch, and V. S. Adamchik, Universality of finite-size corrections to the number of critical percolation clusters, *Phys. Rev. Lett.* **79** (1997), 3447–3450. arXiv:cond-mat/9707168.

[3] S. Mertens, I. Jensen, and R. M. Ziff, Universal features of cluster numbers in percolation, *Phys. Rev. E* **96** (2017), 052119. arXiv:1602.00644.

[4] M. F. Sykes and J. W. Essam, Exact critical percolation probabilities for site and bond problems in two dimensions, *J. Math. Phys.* **5** (1964), 1117–1127. doi:10.1063/1.1704215.

[5] T. Antunović and I. Veselić, Sharpness of the phase transition and exponential decay of the subcritical cluster size for percolation on quasi-transitive graphs, *J. Stat. Phys.* **130** (2008), 983–1009. arXiv:0707.1089.

[6] L. Russo, On the critical percolation probabilities, *Z. Wahrscheinlichkeitstheorie verw. Gebiete* **56** (1981), 229–237. doi:10.1007/BF00535742.

[7] G. R. Grimmett, On the number of clusters in the percolation model, *J. London Math. Soc.* (2) **13** (1976), 346–350. Author's copy.

[8] R. Mansour, Counting clusters in a coloring grid, *Discrete Math. Lett.* **5** (2021), 20–23. doi:10.47443/dml.2021.0002.

[9] N. Berrocal Huamaní, Bipartite noncrossing Frontier states for cluster enumeration on rectangular grids, *Open J. Math. Sci.* **10** (2026), 1230–1247. doi:10.30538/oms2026.0343.

[10] J. van den Berg and A. Ermakov, A new lower bound for the critical probability of site percolation on the square lattice, *Random Structures Algorithms* **8** (1996), 199–212. Author's copy.